The influence of moisture on the energy performance of retrofitted walls

Mafalda Amorim[1], *Vasco Peixoto de* Freitas[1], *Isabel* Torres[2], *Tomasz* Kisilewicz[3] and *Umberto* Berardi[4]

[1] University of Porto, CONSTRUCT-LFC, Faculty of Engineering (FEUP), Portugal
[2] University of Coimbra DEC-FCTUC, ADAI-LAETA, Itecons, Portugal
[3]Cracow University of Technology, Poland
[4]Ryerson University, Toronto, Canada

Abstract. The renovation of old building facades should be performed mainly considering the building energy demand reduction. For this purpose, it is necessary to select retrofitted solutions that should be able of minimizing heat losses through walls. However, it is not only the nominal thermal transmittance that influences the amount of heat transported through the wall, but also the moisture content within the walls under in-service conditions. The main objective of this paper is the evaluation of the influence of the moisture content on the energy performance of retrofitted walls. A numerical study using the software WUFI Pro was carried out to quantify the influence of wind driven rain on the thermal transmittance of different wall assemblies exposed to different climates and orientations. This study reports the transient thermal transmittance of different retrofitted wall solutions as a function of moisture content.

1 Introduction

The renovation of old building facades should be performed on the basis of the reduction of energy consumption in order to reduce the building energy demand and the related greenhouse gas emissions. For this purpose, it is necessary to select a retrofitted solution capable of minimising heat losses through the walls. However, it is not only the retrofitted solution of the wall that influences the amount of heat transported through it, but also the moisture content of the walls under in-service conditions.

The energy performance of exterior walls can be considerably worsened by the presence of moisture content in porous layers. For certain building materials, thermal conductivities are significantly affected by moisture. When porous material pores are filled with water, their thermal conductivities increase [1-6]. Consequently, the currently calculated thermal transmittance values from the "dry" conductivities (very low moisture content) may not be accurate if the walls are wet. As a matter of fact, several experimental and numerical studies have investigated the effect of moisture on the thermal transmittance values of different walls and concluded that the increase in moisture content in a wall can considerably increase the thermal transmittance values [7-12].

The main goal of this study is to quantify the influence of climate conditions on the non-steady thermal transmittance of retrofitted walls. Based on numerical simulations, this

paper evaluates the impact that Porto and Kraków climates have on the energy performance of a brick massive masonry wall without insulation, outfitted with a traditional interior insulation system with different insulation thicknesses and without exterior plaster. The impact of wind-driven rain (WDR) on the energy behaviour of the walls is evaluated too. The analysis is performed for both West and South-orientated walls.

In the next section, the methodology is described. Then, an overview of the results is provided paying attention to the water content profiles, heat flux and non-steady thermal transmittance. To finish, the main conclusions are summarised in section 4.

2 Methodology

The influence of moisture on the dynamic energy performance of retrofitted walls exposed to different climates is quantified. Following the simulation model, the investigated wall configurations and the boundary conditions are described.

2.1 Hygrothermal model for the numerical simulation

To study the hygrothermal performance of the wall configurations under real climatic conditions, the coupled heat and moisture transfer in the building components is simulated with WUFI Pro. The program takes into account heat transport by thermal conduction, enthalpy flows with phase change, short-wave solar radiation and night-time long-wave radiation cooling. The vapour transport mechanisms included are vapour diffusion and solution diffusion. The liquid transport mechanisms included are capillary conduction and surface diffusion.

For coupled heat and mass transfer for vapour diffusion, liquid flow, and thermal transport in parts of the envelope, the model solves the following equations [13]:

$$\frac{dH}{d\vartheta}\cdot\frac{\partial\vartheta}{\partial t} = \nabla\cdot(\lambda\nabla\vartheta) + h_v\nabla\cdot\left(\delta_p\nabla(\varphi p_{sat})\right) \quad (1)$$

$$\frac{dw}{d\varphi}\cdot\frac{\partial\varphi}{\partial t} = \nabla\cdot\left(D_\varphi\nabla\varphi + \delta_p\nabla(\varphi p_{sat})\right) \quad (2)$$

where $\frac{dH}{d\vartheta}$ is the heat storage capacity of the moist building material (J/m^3 K), $\frac{dw}{d\varphi}$ is the moisture storage capacity of the building material (kg/m^3), λ is the thermal conductivity of the moist building material (W/m K), D_φ is the liquid conduction coefficient (kg/ms), δ_p is the water vapour permeability (kg/msPa), h_v is the evaporation enthalpy of the water (J/kg), p_{sat} is the water vapour saturation pressure (Pa), ϑ is the temperature (K) and φ is the relative humidity.

The temperature and relative humidity are the driving potentials of the flux. On the left-hand side of equation 1 and 2 are the storage terms while the fluxes on the right-hand side in both equations depend on the local temperature and humidity conditions [14].

2.2 Wall configurations and material properties

In a first step, three wall assemblies were investigated. These walls consist of a 2-cm-thick layer of external plaster, a 38-cm-thick solid brick masonry wall and a 2-cm-thick layer of lime plaster. The masonry layer is simplified in a single isotropic brick layer, neglecting the mortar joints. Therefore, a one-dimensional simulation is enough. This simplification is validated for the current study, as shown in [15]. The interior insulation systems applied to

the walls consist of mineral wool coated with gypsum board. Table 1 presents the cross section of the walls and the corresponding dry thermal transmittances at 50% relative humidity, calculated as described in [16].

Table 1. Cross section and properties of the simulated walls.

code	cross section of the simulated walls.	layers and U-value (in dry condition)
w1	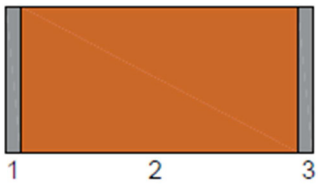	1 - exterior plaster (2 cm) 2 - solid brick masonry (38 cm) 3 - lime plaster (2 cm) U_{dry} = 1.20 W/(m^2 K)
w2	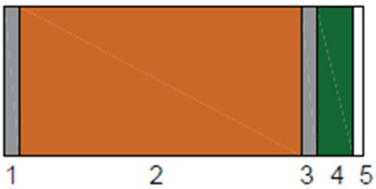	1 - exterior plaster (2 cm) 2 - solid brick masonry (38 cm) 3 - lime plaster (2 cm) 4 - mineral wool (5 cm) 5 - gypsum board (1.25 cm) U_{dry} = 0.47 W/(m^2 K)
w3	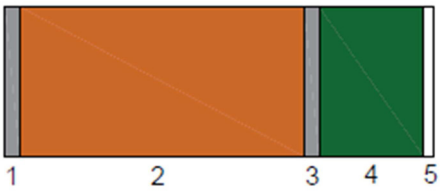	1 - exterior plaster (2 cm) 2 - solid brick masonry (38 cm) 3 - lime plaster (2 cm) 4 - mineral wool (14 cm) 5 - gypsum board (1.25 cm) U_{dry} = 0.23 W/(m^2 K)

The properties of the brick, lime plaster, mineral wool and gypsum board materials used to simulate the hygrothermal performance of the wall assemblies are given in Table 2 and Fig. 1. The WUFI database provided the values for the several properties. Table 2 presents values of bulk density, porosity, specific heat capacity, dry thermal conductivity, water vapour diffusion resistance factor and the capillary water absorption coefficient; Fig. 1 presents the thermal conductivities of the materials as a function of moisture content.

Table 2. Basic material properties used in numerical simulations.

Material	**Bulk density** ρ kg/m^3	**Porosity** ε m^3/m^3	**Specific heat capacity** c J/ (kg K)	**Dry thermal conductivity** λ_0 W/ (m K)	**Water vapour resistance factor** μ -	**Capillary water absorption coefficient** A kg/(m^2 s$^{1/2}$)
Solid brick	1,800	0.31	850	0.60	15	0.05
Lime plaster	1,600	0.30	850	0.70	7	0.05
Mineral wool	60	0.95	850	0.04	1.3	1.3
Gypsum board	850	0.65	850	0.20	8.3	-

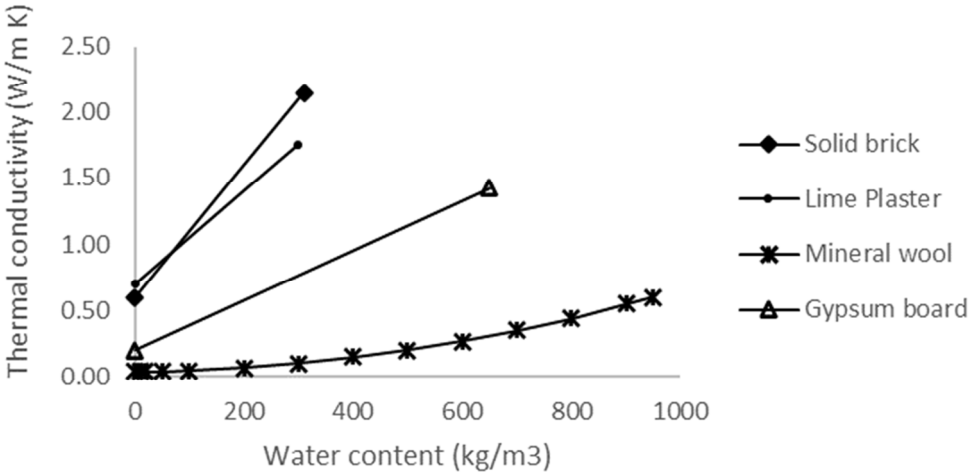

Fig. 1. Thermal conductivities as a function of moisture content.

With regards to the surface transfer coefficients, the conventional values of 0.125 m^2 K/W and 0.06 m^2 K/W are used for the internal and the external surface heat resistance, respectively. The short-wave radiation absorptivity is 0.4 (short-wave radiation absorptivity of a normal bright plaster) if the wall is coated with exterior plaster and 0.68 (short-wave radiation absorptivity of a brick) if the wall is externally uncoated. The long-wave radiation emissivity is 0.9. The rainwater absorption factor is either 0.7 or 0, depending on whether the wall is exposed or not exposed to wind-driven rain, respectively. The adopted initial conditions are constant across the wall section with 80% for relative humidity and 20°C for temperature.

2.3 Boundary conditions

The analysis is performed for the West- and South-orientated walls in Porto, Portugal and in Kraków, Poland. The locations were selected to apply a hygrothermal load with different outdoor temperatures combined with wind-driven rain and solar radiation. For Porto, the average temperature is 15.4°C, the annual amount of wind-driven rain is 275 mm for west orientation and 350 mm for south orientation and the annual amount of solar radiation is 552 kWh/m^2 for west orientation and 900 kWh/m^2 for south orientation. For Kraków, the average temperature is 8.2°C, in the case of the west façade, which is the most exposed to wind, the annual amount of wind-driven rain is 157 mm and the annual amount of solar radiation upon the west-oriented vertical plane is 849 kWh/m^2.

Wind-driven rain on the walls was calculated by wind direction, wind speed and rain according to the method of ASHRAE Standard 160P "Design criteria for moisture control in buildings". The rain exposure factor (FE) and the rain deposition factor (FD) are considered to be 1.0 and 0.5, respectively. These values have been used in other recent studies which looked at the moisture risks of different environmental combination loads for highly insulated walls [17,18].

The indoor conditions were attained through EN 15026, with indoor temperature and relative humidity calculated on the basis of outdoor air temperature. The indoor temperature is kept constant at 20ºC, except when the outdoor temperature exceeds 10ºC, similarly to other studies [17,18]. The indoor relative humidity varies between 30% and 60%. Hourly climate data are used in the simulation.

3 Results and discussion

3.1 Profile of water content

Figure 2 shows the maximum values of moisture density (amount of water in relation to the unit wall area) and the final values of moisture density after five years of simulation. A significant relationship can be observed between the moisture content, the wall orientation and the applied thermal insulation layer. In the case of a building located in Porto, high loads of wind-driven rain lead to a high water content values for both west and south orientations. In the case of a building located in Krakow, wind-driven rain from the west results in even several times the increase of moisture content in relation to the southern orientation. The momentary maximum moisture values show even greater differences. In the case of the western orientation of the wall, the relationship between moisture and the presence of additional thermal insulation is also important. The reduced heat flow through the partition results in poor drying intensity. The moisture level is elevated throughout the year. It should be stated here that only to a small extent is the source of moisture the interstitial condensation of water vapour caused by internal insulation. Based on a comparison of the simulation results of a single-layer wall that is completely protected from wind-driven rain and with the added internal insulation, it can be determined that the maximum increase in moisture caused by this effect is around 1 kg /m^2 of wall.

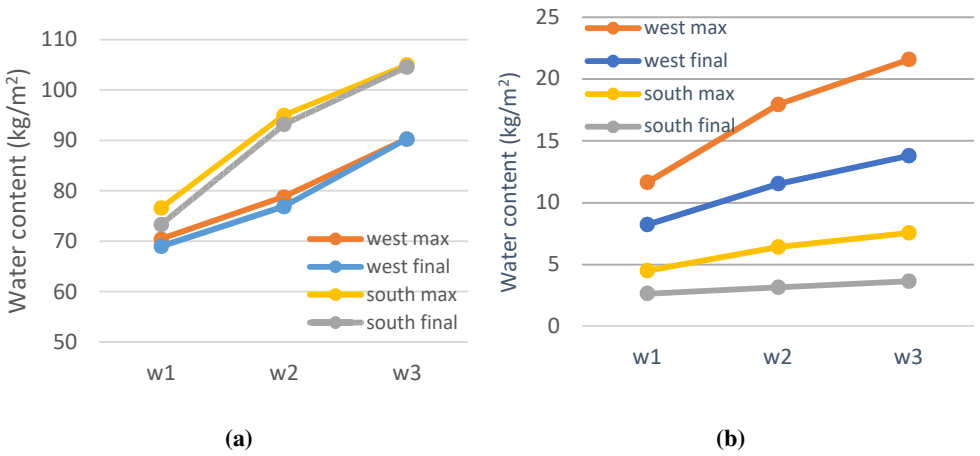

Fig. 2. Water content density (maximum momentary values and final values after 5-year simulation) in the wall located in a) Porto, b) Kraków; water content ranges are different in both diagrams.

Figures 3 and 4 show the water content in the massive brick layer during the entire 5 years simulated period for Porto and Kraków, respectively. The maximum water content in the brick layer in Krakow is over two times lower than in Porto. The initial moisture distribution in the wall quickly equalises and starting from the second year, the annual humidity fluctuations are practically identical. There is no year by year increase of water content. According to previous information, a significant increase in the humidity of the whole wall and brick layer is associated with the inner layer of thermal insulation. It is dependent on the thermal resistance of the added layer.

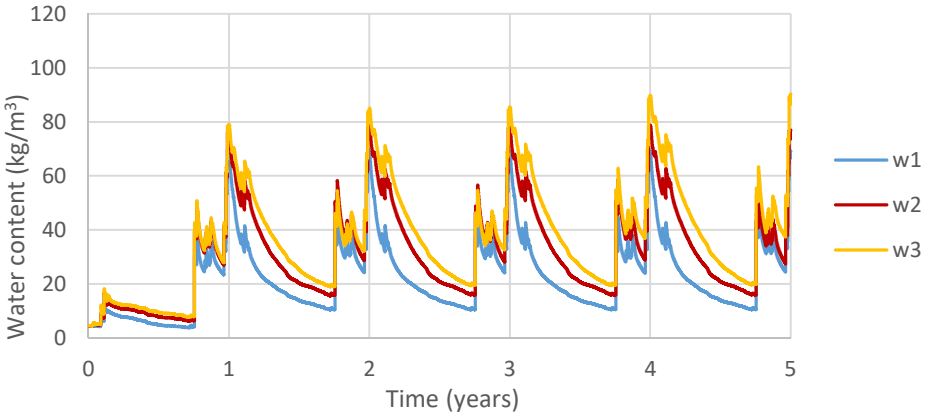

Fig. 3 Water content in the brick layer for the west-orientated walls located in Porto exposed to wind driven rain

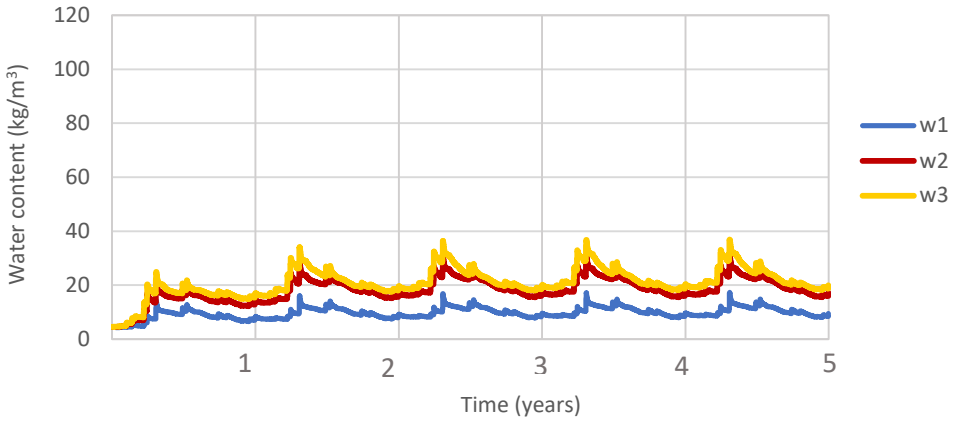

Fig. 4 Water content in the brick layer for the west-orientated wall located in Krakow exposed to wind driven rain

3.2 Thermal transmittance under non-steady conditions

The impact of wind-driven rain on wall humidity and its thermal resistance is very significant and strongly associated with the local climatic conditions. Table 3 presents the transient thermal transmittances of the walls, the variation between the thermal transmittances of the walls exposed and not exposed to wind-driven rain and the energy losses through the walls for the Porto and Kraków climates.

In the case of a poorly insulated brick wall and a large amount of wind-driven precipitation in Porto, the increase in associated heat losses can be very high and exceeds 40%. The reduced effects of wind in Krakow, despite much harsher temperature conditions, result in an increase of heat losses of around 8%. As previously shown, due to the applied internal insulation, the moisture content of brickwork increases. However, due to the increased thermal resistance of the total assembly, the importance of the thermal resistance of the brickwork decreases and the impact of moisture content on heat loss in Porto is reduced to around 20-25%, and to only a few per cent in Krakow. Due to local climate

conditions and the strong influence of the ocean, the wall orientation has only a limited effect on heat losses reduction in Porto, in Krakow, this effect seems to be obvious.

Table 3 Thermal transmittance and heat losses.

Wall configuration	Orientation	Exposure to rain	Porto			Kraków		
			U transient ($W/m^2 K$)	Variation	Energy losses (kWh/m^2 year	U transient ($W/m^2 K$)	Variation	Energy losses (kWh/m^2 year
w1	West	Yes	1.79	40.9 %	99	1.29	6.6%	141
		No	1.27		76	1.21		131
	South	Yes	1.64	53.3 %	93	1.18	0.8%	128
		No	1.07		66	1.17		127
w2	West	Yes	0.61	19.6 %	38	0.51	5.4%	56
		No	0.51		31	0.48		53
	South	Yes	0.54	25.6 %	35	0.47	0.6%	52
		No	0.43		27	0.47		51
w3	West	Yes	0.28	12.0 %	18	0.24	3.9%	29
		No	0.25		15	0.23		26
	South	Yes	0.25	19.0 %	16	0.228	0.1%	27
		No	0.21		13	0.226		25

4 Conclusions

The simulation analyses presented in this article concerned the impact of local climate conditions on the moisture content and energy performance of building walls. Based on the results, the following conclusions can be summarized:

- The building envelope designer should take into account wind-driven rain because it may cause a significant increase in moisture content of the wall materials and an increase in heat loss. However, the scale of changes, strongly depends on the local climate (above 40% in Porto and 8% in Krakow), so the solutions used should also be sensitive to each case.
- The orientation of the wall and its possible protection against wind is of great importance for the course of this phenomenon. Therefore, it makes sense to use, solutions that separate the structure from the external environment and various other solutions depending on the wall orientation.
- The improvement of the thermal resistance of traditional walls from the inside increases the average moisture level of the masonry layer throughout the year, posing a potential threat to wall durability. This is mainly the result of the slower drying of rainwater.
- Internal thermal insulation without the use of vapour barrier is also associated with the periodic condensation of water vapour in a multi-layer wall. However, the amount of water resulting from this process is small, around 3% in relation to the amount of rainwater. Nevertheless, it is necessary to check in the forthcoming works whether the local moisture content in individual materials would cause their destruction.

References

1. M. Kumaran. *Heat, Air and Moisture Transfer in Insulated Envelope Parts Task 3: Material properties* (1996)
2. M. Jerman and R. Černy, Energ. Buildings **53**, 39-46 (2012)
3. F. Szodrai and A. Lakatos, Environ. Eng. Manag. J. **13** (11), 2881-2886 (2014)
4. M. Gomes, I. Flores-Colen, L. Manga, A. Soares and J. Brito, Constr. Build. Mater. **135**, 279-286 (2017)
5. V. Kočí, E. Vejmelková, M. Čáchová, D. Koňáková, M. Keppert, J. Maděra and R. Černý, Int. J. of Thermophys. **38** (2), 28 (2017)
6. J. Maia, N. Ramos and R. Veiga, Build. Environ. **144**, 437-449 (2018)
7. V. De Freitas, *Transferência de humidade em paredes de edifícios análise do fenómeno de interface.* (Portugal 1992)
8. U. Berardi, Energy **182**, 777-794 (2019).
9. A. Lakatos and U. Berardi, Int. Rev. Appl. Sci. Eng. **9** (2), 163-168 (2018).
10. E. Vereecken and S. Roels, Mater. Struct. **48** (9), 3009-2021 (2015)
11. G. Coelho and F. Henriques, J. Build Eng **7**, 121-132 (2016)
12. P. Alonso Alonso, *An experimental and numerical study of hygrothermal behaviour of an open-joint ventilated façade in Northwest Iberian Peninsula*. PhD Thesis. Universidad da Coruña (2017)
13. H. Künzel, *Simultaneous heat and moisture transport in building components. One- and two-dimensional calculation using simple parameters.* (Stuttgart 1995)
14. A. Holm, J. Radon, H. Künzel and K. Sedlbauer, *Description of the IBP holistic hygrothermal model.* IEA Annex 41. Zurich, Switzerland (2004)
15. E. Vereecken and S. Roels, Constr. Build. Mater. **41,** 697-707 (2013)
16. EN ISO 6946 (2007)
17. K. Gradeci, U. Berardi, B. Time and J. Köhler, Energ. Buildings **177**, 112-124 (2018)
18. K. Gradeci and U. Berardi, J. Build. Phys. **43** (3), 187-207 (2019)